

Effect on AC Conductivity of Nanocrystalline Spinel Ferrite Material due to Substitution of Ni^{2+} , Co^{2+} and Cu^{2+} in CuCo , NiCu and CoNi Respectively Prepared by Sol Gel Auto Combustion Method

A.M. Tamboli¹, Dr. Mazahar Farooqi³, Dr. Gulam Rabbani²

Associate Professor, Department of Electronic Science, Poona College, Pune, Maharashtra, India¹

Associate Professor, Department of Physics and Electronics, Maulana Azad College, Aurangabad, Maharashtra, India²

Associate Professor, Department of Chemistry, Dr. Rafiq Zakaria College for Women, Navkhanda, Aurangabad, Maharashtra, India³

ABSTRACT: Herein, the Dielectric properties such as AC Conductivity (σ_{ac}) are reported for the nanocrystalline spinel ferrite material in the series of $[\text{Ni}_x \text{Cu}(\text{constant}) \text{Co}_{0.8-x} \text{Fe}_2\text{O}_4]$, $[\text{Co}_x \text{Ni}(\text{constant}) \text{Cu}_{0.8-x} \text{Fe}_2\text{O}_4]$ and $[\text{Cu}_x \text{Co}(\text{constant}) \text{Ni}_{0.8-x} \text{Fe}_2\text{O}_4]$ where constant=0.2 with $x=0.2, 0.4$ and 0.6 synthesized by using AR grade metal nitrates with the help of Sol-Gel auto-combustion technique. The variation in the AC Conductivity is studied at room temperature by using the LCR Meter in the frequency range of 100 Hz to 5MHz. The effect on AC Conductivity due to the substitution of Ni^{2+} , Co^{2+} and Cu^{2+} density 'x' in $[\text{Ni}_x \text{Cu}(\text{constant}) \text{Co}_{0.8-x} \text{Fe}_2\text{O}_4]$, $[\text{Co}_x \text{Ni}(\text{constant}) \text{Cu}_{0.8-x} \text{Fe}_2\text{O}_4]$ and $[\text{Cu}_x \text{Co}(\text{constant}) \text{Ni}_{0.8-x} \text{Fe}_2\text{O}_4]$ respectively is discussed. The nanocrystalline spinel Structural of ferrite material is confirmed by Fourier Transform Infrared Spectroscopy (FT-IR) and Scanning Electron Microscope (SEM). The presence of metal nitrates is confirmed by Energy Dispersive X-Ray Spectroscopy (EDX).

KEYWORDS: Sol-gel auto-combustion, LCR meter, FT-IR, SEM and EDX.

I. INTRODUCTION

The dielectric properties of nanocrystalline ferrite materials make them suitable for magnetic storage devices and high frequency applications in the field of electronic science and communication technology. The ferrite material of specific AC conductivity is also used to reduce electromagnetic noise, frequency filters and electric spike absorber. It is also used in fabricating light weight transformer and in various frequency filters. Frequency ferrites are widely used in microwave devices such as insulators, circulators, and phase splitter and shifters because of their high resistivity, low eddy current loss and excellent magnetic properties. The general formula of ferrite is MFe_2O_4 and magnetic properties of ferrites are dependent on the distribution of metal cation at tetrahedral A-site and at octahedral B-site. Where $\text{M}=\text{Zn}^{2+}$, $\text{M}=\text{Cu}^{2+}$, $\text{M}=\text{Co}^{2+}$, $\text{M}=\text{Mg}^{2+}$, $\text{M}=\text{Ni}^{2+}$ etc. [1-5].

International Journal of Innovative Research in Science, Engineering and Technology

(An ISO 3297: 2007 Certified Organization)

Website: www.ijirset.com

Vol. 6, Issue 6, June 2017

II. MATERIALS AND METHODS

2.1 Synthesis of ferrite powder

In Sol Gel method the chemical reaction is helping for auto combustion and this process is a self-sustaining combustion synthesis technique and it results in providing fine homogeneous powder of metal-oxide. The sol gel auto combustion process basically takes place in two steps namely (a) Formation of a Gel and (ii) Auto-Ignition. Aqueous precursor solution contains various metal nitrates and fuel such as ascorbic acid, urea, glycine, and citric acid. This solution was heated until the excess water is removed by evaporating. Here citric acid is used as fuel. At the end of chemical reaction the viscous liquid foam gets ignited and undergoes self-sustained combustion and produces ashes containing the oxide product. Very large amount of heat is generated during combustion process in the form of either fire or a flame and therefore, the process is called as auto combustion process. External heat is given by using hot base plate at 100°C, till the formation of gel. When ignition starts at that time dried gel burnt in a self-propagating combustion manner until all gels were completely burnt out to form a fluffy loose structure and converted in to fluffy ash as shown in Fig. 1 and Fig. 2.

In auto combustion reaction the energy is supplied itself due to fuel citric acid. During the auto combustion process Gases such as CO₂, H₂O and N₂ gets evolve, and formation of fine particle ashes takes place. The auto combustion method uses the energy produced by the exothermic decomposition of a redox mixture of an organic compound with metal nitrates. In the combustion organic compounds, nitrates and mixture behave like conventional oxidants and fuels. Very huge amount of heat of combustion (or flame temperature) helps in crystallization and formation of the required phase. The properties of the final product in the form of ash such as surface area, particle size and porosity depend on the method of combustion. The departure of gases helps the desegregation of the products due to which porosity increases and heat dissipation also takes place due to departure of gases. Exothermicity of combustion is controlled by the ratio of oxidizer to fuel and nature of the fuel used in chemical reaction [6-10].

Without the use of costly and expensive high temperature furnaces this technique produces a homogeneous product in a very short amount of time. Auto combustion synthesis reaction can be influenced by many parameters such as the fuel-to-oxidizer ratio, the type of fuel, the ignition temperature and the hardness of water of the precursor mixture. The fuel to oxidizer ratio also plays a very important role in influencing the reaction and reducing the time. A way to control the flame temperature of the reaction is by varying the ratio of fuel to oxidizer.

The elemental stoichiometric coefficient, ϕ_e , is used to control the ratio of fuel to oxidizer in the reaction. ϕ_e represents the ratio between the oxidizing and reducing components of the metal nitrate fuel mixture. When ϕ_e is less than one ($\phi_e < 1$) it is fuel rich and when ϕ_e is greater than one ($\phi_e > 1$), the mixture does not have enough fuel for the completion of reaction. Fig. 3 shows the auto combustion synthesis flow chart used for the synthesis of the ferrite powders.

Ferrite powder is prepared by using sol-gel auto combustion method. Analytical grade Nickel Nitrate [Ni(NO₃)₂.6H₂O], Copper Nitrate [Cu(NO₃)₂.3H₂O], Cobalt Nitrate [Co(NO₃)₂.6H₂O], Iron Nitrate [Fe(NO₃)₃.9H₂O], Citric Acid [C₆H₈O₇.H₂O], Distilled water is prepared in the laboratory using all quick fit glass assembly and liquid ammonia were used as raw materials in sol gel auto combustion method.

The series [Ni_xCu(constant)Co_{0.8-x}Fe₂O₄], [Co_xNi(constant)Cu_{0.8-x}Fe₂O₄] and [Cu_xCo(constant)Ni_{0.8-x}Fe₂O₄] where, constant=0.2 with x= 0.2, 0.4 and 0.6 of ferrites have been prepared in three Sets namely SET-I, SET-II and SET-III using Sol-Gel Auto-combustion method. All the chemicals were from E-mark, India (AR grade with 98% purity to 99.9% purity).

Accurately weighted quantity of Metal nitrates and citric acid is added in to distilled water of 100ml and a solution is prepared. The solution in a glass beaker was homogenized by continuous stirring with the help of magnetic needle by using the instrument so called magnetic stirrer. The magnetic stirrer is having the facility of controlling the revolution per minit (RPM) of magnetic needle as well as temperature of base plate. The acidic or alkaline level (pH) of the solution was adjusted to 7 using liquid ammonia and the solution is continuously heated at 100°C on a hot plate with magnetic stirrer with the help of hard glass beaker. With continuous heating it initially transformed into sol then gel and it requires five to six hours shown. When liquid gets converted in to gel the magnetic needle is removed and gel stick with magnetic needle is used for IR characterization.

International Journal of Innovative Research in Science, Engineering and Technology

(An ISO 3297: 2007 Certified Organization)

Website: www.ijirset.com

Vol. 6, Issue 6, June 2017

The ferrite powder material was sintered in an electrical furnace with super kanthal (MoSi₂) heating elements and alumina insulation boards as chamber walls. The size of the chamber is 250x150x150 mm. The thermal regime of the furnace was controlled through a “Eurotherm” programmer-cum-controller by using microcontrollers with an accuracy of ± 2°C. The already crushed and grounded samples are heated from room temperature to 400°C at a rate 1°C/min followed by a soaking at 400°C for 4 hours.

The ferrite powder was sintered at 400°C for 4 hours in air medium to get better crystallization and homogeneous cation distribution in the spinel and finally ground to get [(Ni_{0.2} Cu_{0.2}Co_{0.6})Fe₂O₄], [(Ni_{0.4} Cu_{0.2}Co_{0.4})Fe₂O₄], [(Ni_{0.6} Cu_{0.2}Co_{0.2})Fe₂O₄], [(Ni_{0.2} Cu_{0.6}Co_{0.2})Fe₂O₄], [(Ni_{0.2} Cu_{0.4}Co_{0.4})Fe₂O₄] and [(Ni_{0.4} Cu_{0.4}Co_{0.2})Fe₂O₄] ferrite powders. Table 1 indicates Label and composition of ferrite materials for all three Sets.

2.2 Perpetration and Sintering of pellets:

The pellets are prepared by mixing the polyvinyl alcohol (PVA) as binder in to ferrite powder. The mixed powder was uniaxially pressed by using a hydraulic press machine by applying the pressure of about 60 kg/cm³ for about 1 minute in a die of 10mm diameter. The final sintering of pellets was carried out at 200°C for about 2 hours in air medium to densify the pellets. The pellets of diameter D_o-10 mm, thickness-2 mm are fabricated. The prepared samples of pellets were sintered in a furnace which uses electricity for heating the chamber with the help of super kanthal (MoSi₂) heating elements and alumina insulation boards as chamber walls. The dimension of chamber is 250x150x150 mm. The thermal regime of the furnace was controlled through a “Eurotherm” programmer-cum-controller designed by using microcontroller with an accuracy of ± 2°C. The compacted samples heated from room temperature to 200°C at a rate 1°C/min followed by a soaking at 200°C for 2 hrs for binder burnout. The pellets are shown in Fig. 4.

2.3 Characterization of AC conductivity (σ_{ac}).

The dielectric constant (ε'), dielectric loss tangent (tan δ) and AC conductivity (σ_{ac}) of prepared samples were measured in the frequency range of 100 Hz to 5 MHz by using impedance analyser meter at room temperature. The data acquisition system of digital impedance analyser (LCR meter) provides the information of applied frequency (f), measured Series Capacitance (Cs), Parallel Capacitance (Cp), Quality factor (Q).

The data provided by digital impedance analyser meter and the available reading such as thickness of pellet, d=0.002 meter, Diameter of pellet= 10 millimetre and Area of pellet = π r² = 3.14*.005*.005 meter²=0.0000785 meter² is used for calculations for real part of dielectric constant (ε'), dielectric loss tangent (tan δ) and AC Conductivity. The logarithm of frequency (Log₁₀ f) is taken in to consideration while plotting the graph of (Log₁₀ f) verses any other parameter. Following equations are used

$$\text{Dielectric loss tangent} = (\tan \delta) = 1/Q = \epsilon'' / \epsilon' - (1)$$

$$\text{Dielectric constant (Real Part)} = \epsilon' = C_p * d / \epsilon_0 * A - (2)$$

$$\text{Dielectric constant (Imaginary Part)} = \epsilon'' = (\tan \delta) * \epsilon' - (3)$$

$$\text{AC electrical conductivity} = \sigma_{ac} = 2\pi f * \epsilon_0 * \epsilon' * (\tan \delta) = \omega * \epsilon_0 * \epsilon' * (\tan \delta) - (4)$$

III. RESULTS AND DISCUSSIONS

3.1 AC conductivity (σ) at different concentration of Ni²⁺ ions (A, Band C):

The variation of AC conductivity with the frequency at different concentration of Ni²⁺ ions is shown in Fig. 5. It shows that the AC conductivity decreases with increase in x substitution of Ni²⁺. With the increase in the concentration of Ni²⁺ ions (x), the hopping action of charge carriers decreases due to the decreased concentration of Fe³⁺ ions at B-site. From Fig. 5, it is observed that for x=0.2 (sample A) graph shown by square dots (Black) is having the maximum AC Conductivity and AC Conductivity decreases with the increase in x=0.4 (sample B) and for x=0.6 (sample C) which is shown by circular dots (Red) and triangular dots (Blue) respectively.

International Journal of Innovative Research in Science, Engineering and Technology

(An ISO 3297: 2007 Certified Organization)

Website: www.ijirset.com

Vol. 6, Issue 6, June 2017

The increase in the AC conductivity with frequency is also understood by the hopping model. As the frequency of the applied electric field increases, the hopping frequency of electrons between Fe^{3+} – Fe^{2+} ions at adjacent octahedral site also increases, leading to increase in the conductivity [11-15]. Table 2, shows the values of AC Conductivity for substitution x of Ni^{2+} at 5 MHz.

3.2 AC conductivity (σ) at different concentration of Co^{2+} ions (D, E and A):

From Fig. 6, it is observed that for $x=0.2$ (sample D) graph shown by square dots (Black) is having the minimum AC Conductivity. Here AC Conductivity increases due increase in substitution of Co^{2+} , $x=0.4$ and $x=0.6$ which is shown by circular red dots (sample E) and by triangular blue dots (sample A) respectively.

Table 3, shows the values of AC Conductivity for substitution x of Co^{2+} at 5 MHz.

3.3 AC conductivity (σ) at different concentration of Cu^{2+} ions (D, F and C):

The variation of AC conductivity with the frequency at different concentration of Cu^{2+} ions is shown in Fig. 7. It reveals that the AC conductivity initially increases with increase in x substitution of Cu^{2+} up to $x=0.4$ and then it decreases with further increase in x substitution of Cu^{2+} up to $x=0.6$. With the increase in the concentration of Cu^{2+} ions (x), the hopping action of charge carriers increases due to the increased concentration of Fe^{3+} ions at B-site and further it decreases. Table 4, shows the values of AC Conductivity for substitution x of Ni^{2+} at 5 MHz.

Fig. 7, indicates square dots (Black) for $x=0.2$ is having moderate AC Conductivity in between $x=0.4$ and $x=0.6$, but for $x=0.4$ the circular dots (Red) shows that AC Conductivity increases and thereafter due to further increase in $x=0.6$ AC Conductivity decreases at 5 MHz. This decrease in AC conductivity is shown by triangular dots (Blue). Table 4, shows the values of AC Conductivity for substitution x of Cu at 5 MHz.

It is observed that for all the samples of ferrite material the AC conductivity remains almost constant in the low frequency region and increases abruptly in the high frequency region. Such type of observation is also reported by many researchers. It is well known that the mechanism of the electrical conduction is the same as that of the dielectric polarization [16-18]. Table 5, shows average AC Conductivity for all six samples ferrite material calculated in the range of 100Hz to 5MHz.

The FTIR spectroscopy confirms the single phase nature of the prepared sample. The peak 536.114 cm^{-1} gives the confirmation of Fe_2O_4 . Fig. 8 shows the IR absorption peak at 536.114 cm^{-1} [19-22].

Scanning electron microscope (SEM) images gives the confirmation of particle sizes of around 22–29 nm of $\text{NiCuCo Fe}_2\text{O}_4$ nanoparticles. Fig. 9 shows SEM. A SEM micro graph also shows a uniform grain growth with small pores and high densification at the calcining temperature of 400°C . EDX gives the confirmation about the presence of $\text{NiCuCo Fe}_2\text{O}_4$ in proper proportion. Fig. 10 shows EDX.



Fig. 1: Formation of Gel



Fig. 2: Formation of Ash.

International Journal of Innovative Research in Science, Engineering and Technology

(An ISO 3297: 2007 Certified Organization)

Website: www.ijirset.com

Vol. 6, Issue 6, June 2017

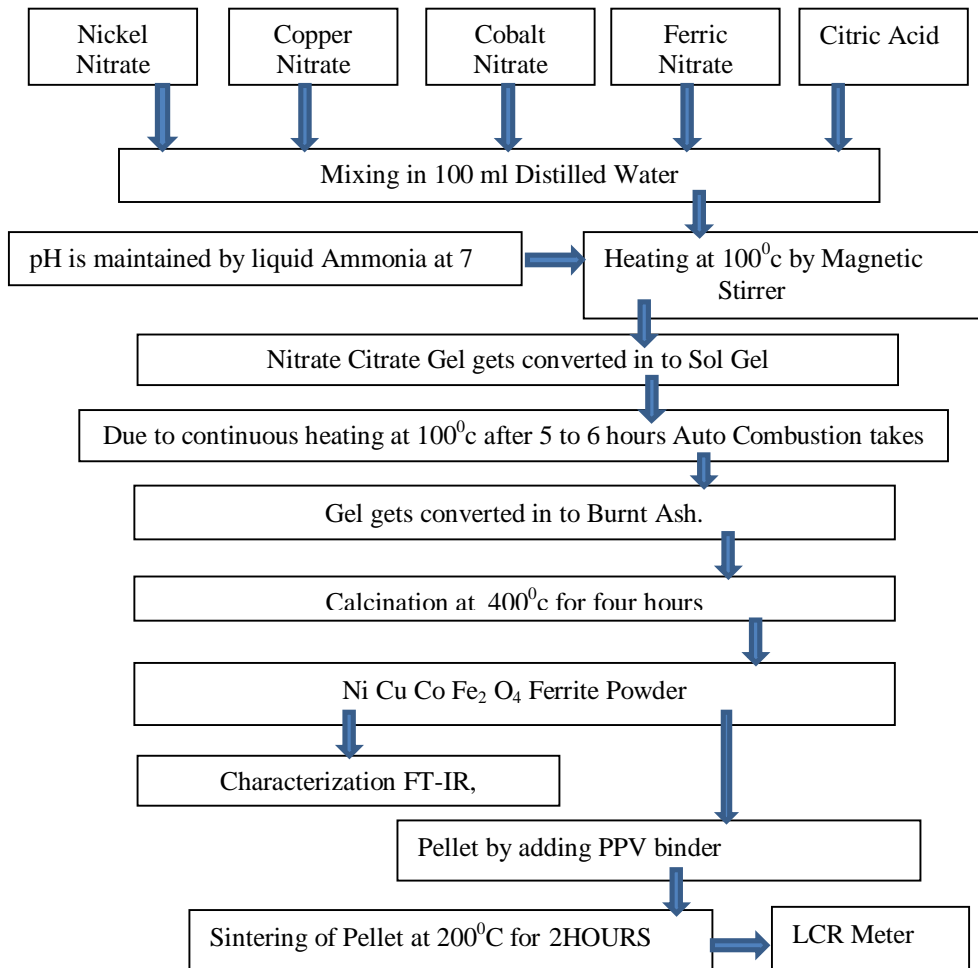


Fig. 3: Flow chart of Sol Gel Method

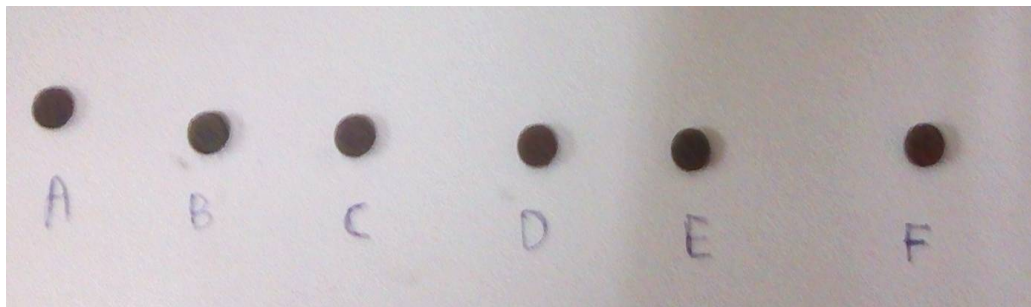


Fig. 4: Pellet Photograph.

International Journal of Innovative Research in Science, Engineering and Technology

(An ISO 3297: 2007 Certified Organization)

Website: www.ijirset.com

Vol. 6, Issue 6, June 2017

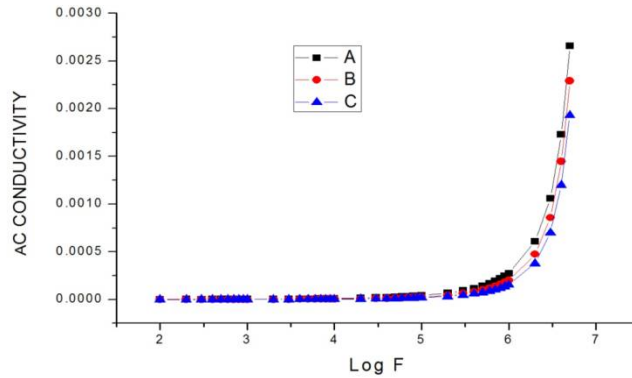


Fig. 5: AC Conductivity for A, B and C.

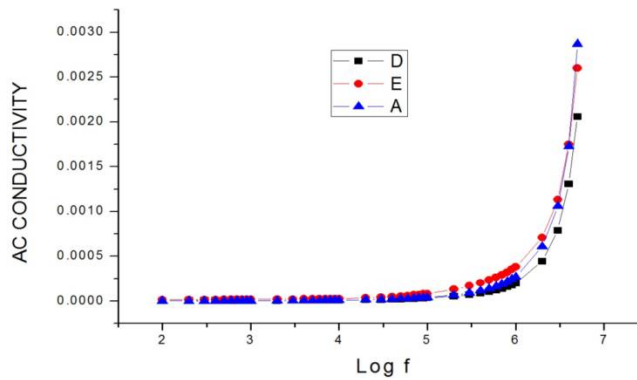


Fig. 6: AC Conductivity for D, E and A.

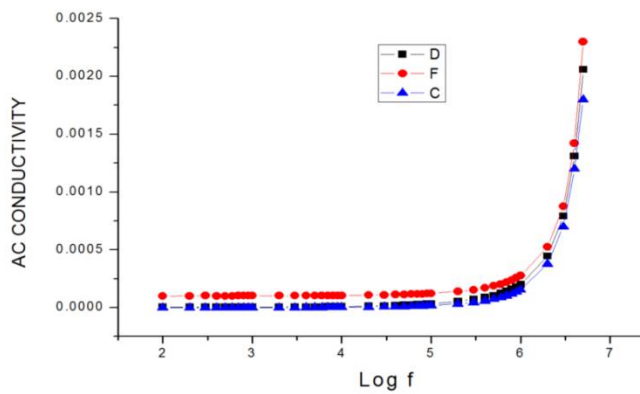


Fig. 7: AC Conductivity for D, F and C.

International Journal of Innovative Research in Science, Engineering and Technology

(An ISO 3297: 2007 Certified Organization)

Website: www.ijirset.com

Vol. 6, Issue 6, June 2017

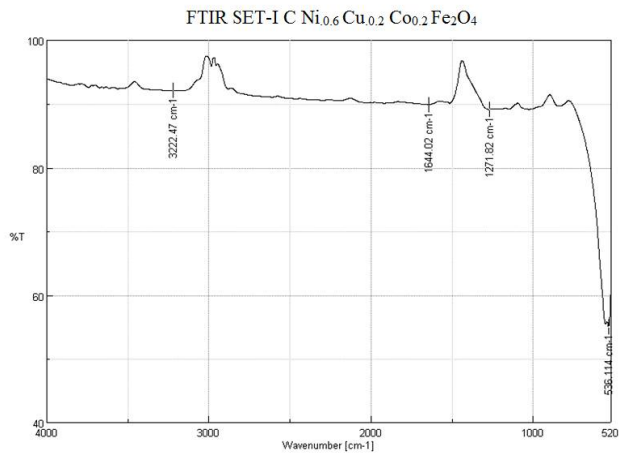


Fig. 8: FTIR graph for SET-I (C)

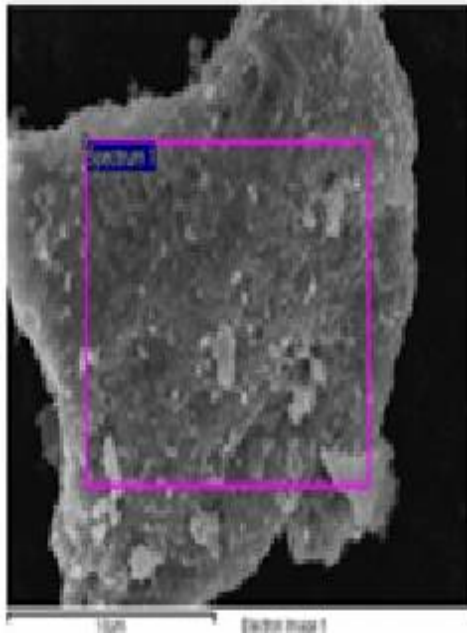


Fig. 9: SEM Photograph.

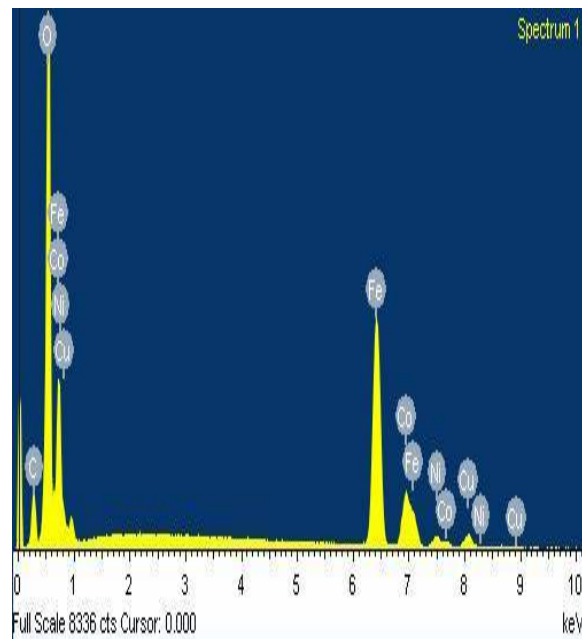


Fig. 10: EDX Photograph.

International Journal of Innovative Research in Science, Engineering and Technology

(An ISO 3297: 2007 Certified Organization)

Website: www.ijirset.com

Vol. 6, Issue 6, June 2017

Table 1: Label and Composition of Ferrite Material.

SET	Label	Ferrite Material
SET-I	A	$[(Ni_{0.2}Cu_{0.2}Co_{0.6})Fe_2O_4]$
	B	$[(Ni_{0.4}Cu_{0.2}Co_{0.4})Fe_2O_4]$
	C	$[(Ni_{0.6}Cu_{0.2}Co_{0.2})Fe_2O_4]$
SET-II	D	$[(Co_{0.2}Ni_{0.2}Cu_{0.6})Fe_2O_4]$
	E	$[(Co_{0.4}Ni_{0.2}Cu_{0.4})Fe_2O_4]$
	A	$[(Co_{0.6}Ni_{0.2}Cu_{0.2})Fe_2O_4]$
SET-III	C	$[(Ni_{0.6}Cu_{0.2}Co_{0.2})Fe_2O_4]$
	F	$[(Ni_{0.4}Cu_{0.4}Co_{0.2})Fe_2O_4]$
	D	$[(Ni_{0.2}Cu_{0.6}Co_{0.2})Fe_2O_4]$

Table 2: AC Conductivity of SET-I.

$[Ni_xCu(\text{constant})Co_{0.8-x}Fe_2O_4], Cu = \text{constant} = 0.2$	
x	AC Conductivity at 5 MHz
(A) For x=0.2	0.002658529
(B) For x=0.4	0.002290749
(C) For x=0.6	0.001927343

Table 3: AC Conductivity of SET-II.

$[(Ni_{(\text{constant})}Cu_{0.8-x}Co_x)Fe_2O_4], Ni = \text{constant} = 0.2$	
x	AC Conductivity at 5 MHz
(D) For x=0.2	0.00206424
(E) For x=0.4	0.00259871
(A) For x=0.6	0.00265852

Table 4: AC Conductivity of SET-III.

$[(Ni_{0.8-x}Cu_xCo_{(\text{constant})})Fe_2O_4], Co = \text{constant} = 0.2$	
x	AC Conductivity at 5 MHz
(D) For x=0.2	0.00206424
(F) For x=0.4	0.00210402
(C) For x=0.6	0.00192734

Table 5: Average AC Conductivity of all samples.

Ferrite	Avg. AC Conductivity
SET-I- A $[(Ni_{0.2}Cu_{0.2}Co_{0.6})Fe_2O_4]$	0.000194143
SET-I- B $[(Ni_{0.4}Cu_{0.2}Co_{0.4})Fe_2O_4]$	0.000155638
SET-I- C $[(Ni_{0.6}Cu_{0.2}Co_{0.2})Fe_2O_4]$	0.000126047
SET-II- D $[(Ni_{0.2}Cu_{0.6}Co_{0.2})Fe_2O_4]$	0.000148797
SET-II- E $[(Ni_{0.2}Cu_{0.4}Co_{0.4})Fe_2O_4]$	0.000231988
SET-III- F $[(Ni_{0.4}Cu_{0.4}Co_{0.2})Fe_2O_4]$	0.000140762

International Journal of Innovative Research in Science, Engineering and Technology

(An ISO 3297: 2007 Certified Organization)

Website: www.ijirset.com

Vol. 6, Issue 6, June 2017

IV. CONCLUSION

We have successfully fabricated the six different types of Nanocrystalline Ferrite materials and successfully implemented Sol Gel Auto combustion method. All ferrite materials exhibit good AC conductivity and it can be used as core in transformer as well as fabricating antenna and in capacitors.

REFERENCES

- [1] C. G. Whinfrey, D. W. Eckort and A. Tauber, *J. Am. Chem. Soc.* 53 (1982) 2722
- [2] C. Caizer, M. Stefanescu, *J. Phys. D. Appl. Phys.* 35 (2002) 3035.
- [3] M.A. Ahmed, S.F. Mansour, M. Afifi, *J. Magn. Magn. Mater.* 324 (2012) 4-10.
- [4] P.S. Aghav, V.N. Dhage, M.L. Mane, D.R. Shengule, R.G. Dorik, K.M. Jadhav, *Physica B: Cond. Matter.* 406(2011) 4350
- [5] K. Byrappa, M. Yoshimura, Handbook of Hydrothermal Technology, Noyes Publications, New Jersey, USA, 2001.
- [6] P. Hermankova, M. Hermanek, R. Zboril, *Eur. J. Inorg. Chem.*, 2010, 1, 110.
- [7] J. Moulder, Handbook of X-ray Photoelectron Spectroscopy (XPS), USA 1995.
- [8] D. L. Pavla, G. L. Lampman, G. S. Krlz, J. R. Vyvyan, Introduction to spectroscopy, Brooks/colecengage learning, 2009.
- [9] K.W. Wagner, *Ann. Phys.* 40 (1913) 817.
- [10] I.T. Rabinkin, Z.I. Novikova, Ferrites, *Izv Acad. Nauk USSR*, Minsk, 1960.
- [11] J.C. Maxwell, Electricity and Magnetism, vol. 1, Oxford University Press, New York (1973), p. 1.
- [12] M. Penchal Reddy, W. Madhuri, N. Ramamanoher Reddy, K.V. Siva Kumar, V.R.K. Murthy, R. Ramakrishna Reddy, Influence of copper substitution on magnetic and electrical properties of MgCuZn ferrite prepared by microwave sintering method, *Mater. Sci. Eng. C* 30 (2010) 1094–1099.
- [13] K. J. Azadmanjiri, H.K. Salehani, M.R. Barati, F. Farzan, Preparation and electromagnetic properties of Ni_{1-x}Cu_xFe₂O₄ nanoparticle ferrites by sol-gel auto-combustion method, *Mater. Lett.* 61 (2007) 84–87.
- [14] M.A. Ahmed, S.F. Mansour, M. Afifi, *J. Magn. Magn. Mater.* 324 (2012) 4-10.
- [15] P.S. Aghav, V.N. Dhage, M.L. Mane, D.R. Shengule, R.G. Dorik, K.M. Jadhav, *Physica B: Cond. Matter.* 406(2011) 4350.
- [16] J. Jing, L. Liangchao, X. Feng, *J. Rare Earths* 25 (2007) 79.
- [17] J. Azadmanjiri, H.K. Salehani, M.R. Barati, F. Farzan, *Mater. Lett.* 61 (2007) 84–87.
- [18] J. Du, Z. Liu, W. Wu, Z. Li, B. Han, Y. Huang, *Mater. Res. Bull.* 40 (2005) 928–935.
- [19] M.R. Anantharaman, S. Sindhu, S. Jagatheesan, K.A. Malini, P. Kurian, *J. Phys. D* 32 (1999) 1801
- [20] T. Nakamura, Y. Okaro, Electromagnetic properties of Mn–Zn ferrite sintered ceramics, *J. Appl. Phys.* 79 (1996) 7129.
- [21] T. Jahanbin, M. Hashim, K. A. Mantori, *J. Magn. Magn. Mater.* 322(2010) 2684-2689.
- [22] G.F. Goya, H.R. Rechenberg, Superparamagnetic transition and local-order in CuFe₂O₄ nanoparticles, *Nanostruct. Mater.* 10 (1998) 1001–1011.